

# Multiple Bosonic Mode Coupling in Electron Self-Energy of $(\text{La}_{2-x}\text{Sr}_x)\text{CuO}_4$

X. J. Zhou<sup>1,2</sup>, Junren Shi<sup>3</sup>, T. Yoshida<sup>1,4</sup>, T. Cuk<sup>1</sup>, W. L. Yang<sup>1,2</sup>, V. Brouet<sup>1,2</sup>, J. Nakamura<sup>1</sup>, N. Mannella<sup>1,2</sup>, Seiki Komiya<sup>5</sup>, Yoichi Ando<sup>5</sup>, F. Zhou<sup>6</sup>, W. X. Ti<sup>6</sup>, J. W. Xiong<sup>6</sup>, Z. X. Zhao<sup>6</sup>, T. Sasagawa<sup>1,7</sup>, T. Kakeshita<sup>8</sup>, H. Eisaki<sup>1,8</sup>, S. Uchida<sup>8</sup>, A. Fujimori<sup>4</sup>, Zhenyu Zhang<sup>3,9</sup>, E. W. Plummer<sup>3,9</sup>, R. B. Laughlin<sup>1</sup>, Z. Hussain<sup>2</sup>, and Z.-X. Shen<sup>1</sup>

<sup>1</sup>*Dept. of Physics, Applied Physics and Stanford Synchrotron Radiation Laboratory, Stanford University, Stanford, CA 94305*

<sup>2</sup>*Advanced Light Source, Lawrence Berkeley National Lab, Berkeley, CA 94720*

<sup>3</sup>*Condensed Matter Sciences Division, Oak Ridge National Laboratory, Oak Ridge, TN 37831*

<sup>4</sup>*Dept. of Complexity Science and Engineering, University of Tokyo, Kashiwa, Chiba 277-856, Japan*

<sup>5</sup>*Central Research Institute of Electric Power Industry, Komae, Tokyo 201-8511, Japan*

<sup>6</sup>*National Lab for Superconductivity, Institute of Physics, Chinese Academy of Sciences, Beijing 100080, China*

<sup>7</sup>*Department of Advanced Materials Science, University of Tokyo, Japan*

<sup>8</sup>*Dept. of Superconductivity, University of Tokyo, Bunkyo-ku, Tokyo 113, Japan*

<sup>9</sup>*Department of Physics and Astronomy, University of Tennessee, Knoxville, TN 37996*

(Dated: February 2, 2008)

High resolution angle-resolved photoemission spectroscopy data along the  $(0,0)-(\pi,\pi)$  nodal direction with significantly improved statistics reveal fine structure in the electron self-energy of the underdoped  $(\text{La}_{2-x}\text{Sr}_x)\text{CuO}_4$  samples in the normal state. Fine structure at energies of  $(40\sim 46)$  meV and  $(58\sim 63)$  meV, and possible fine structure at energies of  $(23\sim 29)$  meV and  $(75\sim 85)$  meV, have been identified. These observations indicate that, in LSCO, more than one bosonic modes are involved in the coupling with electrons.

PACS numbers: 74.25.Jb, 71.18.+y, 74.72.Dn, 79.60.-i

The recent observation of the electron self-energy renormalization effect in the form of a “kink” in the dispersion has generated considerable interest because it reveals a coupling of the electrons with a collective boson mode of the cuprate superconductors[1]. However, the nature of the bosons involved remains controversial mainly because the previous experiments can only be used to determine an approximate energy of the mode and this energy is close to both the optical phonon[2, 3] and the spin resonance[4]. Determining the nature of the mode(s) that couple to the electrons is likely important in understanding the pairing mechanism of superconductivity.

In conventional superconductors, identification of the fine structure for the phonon anomalies in the tunnelling spectra has played a decisive role in reaching a consensus on the nature of the bosons involved[5]. The fine structure provides fingerprints for much more stringent comparison with known boson spectra. So far, such fine structure has not been detected in the angle-resolved photoemission spectroscopy (ARPES) data. In this Letter we present significantly improved high resolution ARPES data of  $(\text{La}_{2-x}\text{Sr}_x)\text{CuO}_4$  (LSCO) that, for the first time, reveal fine structure in the electron self-energy, demonstrating the involvement of multiple boson modes in the coupling with electrons.

The photoemission measurements were carried out on beamline 10.0.1 at the ALS, using Scienta 2002 and R4000 electron energy analyzers. As high energy resolution and high data statistics are crucial to identify fine structure in the electron self-energy, the experimental conditions were set to compromise between these two

conflicting requirements. The measurement is particularly challenging for LSCO system because of the necessity to use a relatively high photon energy (55eV). Different energy resolution between 12 and 20 meV was used for various measurements on different samples, and the angular resolution is 0.3 degree. An example of the high quality of the raw data is shown in Figs. 1a and 1b. Due to space charge problem, the Fermi level calibration has a  $\pm 5$  meV uncertainty. We mainly present our data on the heavily underdoped LSCO  $x=0.03$  (non-superconducting), LSCO  $x=0.063$  ( $T_c=12$  K) and LSCO  $x=0.07$  ( $T_c=14$  K) samples. These heavily underdoped LSCO samples are best candidates because they exhibit a stronger band renormalization effect above  $T_c$ [3]; a relatively large magnitude of the real self-energy makes the identification of the fine structure easier. The LSCO single crystals are grown by the travelling solvent floating zone method[6]. The samples were cleaved *in situ* in vacuum with a base pressure better than  $4\times 10^{-11}$  Torr. The measurement temperature was  $\sim 20$  K so all samples were measured in the normal state.

Fig. 1c shows the energy-momentum dispersion relation along the  $(0,0)-(\pi,\pi)$  nodal direction extracted by the MDC (momentum distribution curves) method. Because of the larger band-width along the nodal direction, the MDC method can be reliably used to extract high quality data of dispersion in searching for fine structures. It has also been shown theoretically that this approach is reasonable in spite of the momentum-dependent coupling if we are only interested in identifying the mode energies[7]. As seen in Fig. 1c, there is an abrupt slope change (“kink”) in the dispersions for LSCO samples

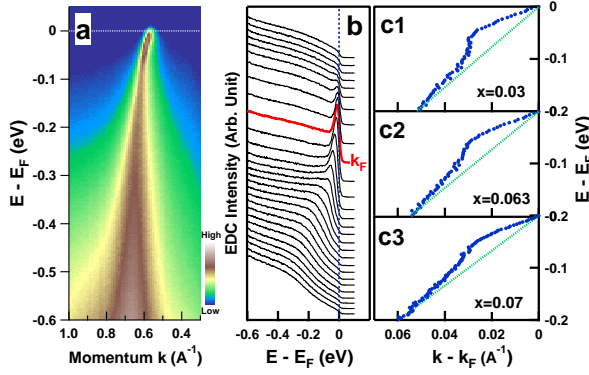


FIG. 1: (a) Raw data of a two-dimensional image showing the photoelectron intensity as a function of momentum and energy for LSCO  $x=0.063$  sample. The intensity is represented by the false-color. The measurement was taken along the  $(0,0)-(\pi,\pi)$  nodal direction at a temperature of  $\sim 20$  K. (b) The photoemission spectra (energy distribution curves, EDCs) for the LSCO  $x=0.063$  sample corresponding to Fig. 1a. The spectrum at the Fermi momentum  $k_F=(0.44\pi/a, 0.44\pi/a)$  (red curve) shows a sharp peak. (c) The energy-momentum relation determined from MDC method for LSCO  $x=0.03$  (c1),  $x=0.063$  (c2) and  $x=0.07$  (c3) samples. The green dashed lines connecting the two points at the Fermi energy and  $-0.2$  eV are examples of a simple selection of the bare band.

with different dopings, similar to that reported before[3]. However, the new data with improved statistics indicates that the “kink” has fine structure and subtle curvatures in it, as seen for example in the LSCO  $x=0.03$  sample (Fig. 1c1).

Since the bare dispersion is expected to be smooth in such a small energy window, the “kink” and its fine structure represent effects associated with the electron self-energy. The real part of the electron self-energy,  $\text{Re}\Sigma$ , can be extracted from the measured dispersion (as in Fig. 1c) by subtracting the “bare dispersion”. Following the convention[8, 10], within a small energy range near the Fermi level, the “bare dispersion” can be assumed as  $\epsilon_0(k)=\alpha_1(k-k_F)+\alpha_2(k-k_F)^2$ . As we will describe later, the values of  $\alpha_1$  and  $\alpha_2$  are determined so as to yield the best fit of the measured dispersion from the maximum entropy method (MEM); the choice of smooth bare band has little effect on the fine structure that originate from the abrupt change in the dispersion. The “effective”  $\text{Re}\Sigma$  for LSCO at various doping levels is shown in Fig. 2a. Also note the data were taken at different energy resolutions, using different analyzers and under different measurement conditions, as described in the caption of Fig. 2.

As seen from Fig. 2a, even with the most optimal experimental conditions we can achieve and in these samples that exhibit the strongest self-energy effects, there remains considerable noise in the data statistics. How-

ever, by searching for peaks or curvature changes, we can clearly identify some fine structure in the data. Two clear features are around  $40\sim 46$  meV and  $58\sim 63$  meV, as indicated by arrows in Fig. 2a, which show up clearly in  $x=0.03$  (Fig. 2a1) and  $\sim 0.06$  samples (Fig. 2a4), although less clearly in  $x=0.063$  and  $x=0.07$  samples. There may be another structure near  $23\sim 29$  meV, which shows up mainly as a shoulder that is visible in  $x=0.03$  (Fig. 2a1),  $0.063$  (Fig. 2a2),  $0.07$  (Fig. 2a3) and possibly in  $x=\sim 0.06$  sample (Fig. 2a4). While these fine features are subtle and one may argue about individual curves, the fact that we have invariably observed them near similar energies in many different samples and under different measurement conditions make the presence of the fine structure convincing.

A natural question is whether the fine structure can be due to instrumental artifact which may be related to detector inhomogeneity and/or system noise. The detector problem can be ruled out because: (1). The data were taken using the “swept mode” of the electron analyzer, i.e., each energy point was averaged over the entire detector range along the energy direction. Therefore, all the energy points for the same angle were taken under the same condition. (2). The inhomogeneity along the angle direction is also minimized by normalizing the photoemission spectra with the spectral weight above the Fermi level which comes from the high harmonics of synchrotron light and is angle-insensitive. (3). Among different measurements, the corresponding detector angle with respect to the dispersion bands vary due to slight changes in measuring geometry. The fact that we observed consistent results suggest that the results are intrinsic; (4). We have carried out our measurements using different analyzers, from SES2002 to the latest R4000, yielding qualitatively similar results. One can also rule out the possibility of noise because they are supposed to be random. But for many different measurements on different samples and under different experimental conditions, the multiple structures are similar in energy within the uncertainty caused by data statistics[9].

The direct inspection in the raw data (Fig. 2a) has clearly established the existence of fine structure in the electron self-energy. This is independent of any models that are used in the data analysis, including the MEM method we use below. In order to better quantify the characteristic energies of these fine features, we take an approach to fit a smooth curve through the measured  $\text{Re}\Sigma$  data and then perform second-order derivative to the fitted curve. Given the statistics level in the data, a spline through the data is difficult because it is somewhat subjective. The MEM procedure, which has been exploited to extract the spectral features of the electron-phonon coupling from ARPES data for the two-dimensional surface state of Be[10], is well suited for this purpose. By incorporating *prior* knowledge, including positiveness of the bosonic function, and zero value of

the bosonic function at zero frequency and above a maximum frequency of 100meV, the MEM is robust against the random noise in the data, insensitive to the fitting details, and is therefore more objective[10]. Since it remains unclear whether the method developed for conventional metal can be extended to cuprate superconductors, as the first step, we use it only as a procedure for curve fitting.

The fitted curves are shown in Fig. 2a together with the measured  $\text{Re}\Sigma$ ; the corresponding second-order derivative of the fitted curves are shown in Fig 2b. As expected, two dominant features near 40~46 meV and 58~63 meV, and one possible feature near 23~29, have been resolved in Fig. 2b. This is consistent with the fine structure identified to a naked eye in the raw data of the electron self-energy (Fig. 2a). In addition, this data analysis process also allows us to identify one more possible feature that may exist at high energy near 75~85 meV, which seems to get stronger with increasing doping. We note that, while the agreement is not perfect at this stage, there is sufficient similarity to suggest the detection of multiple modes.

The fine structure in the electron self-energy originates from the underlying bosonic spectral function. The multiple features in Fig. 2b show marked difference from the magnetic excitation spectra measured in LSCO which is mostly featureless and doping dependent[11]. In comparison, the features in Fig. 2b show more resemblance to the phonon density-of-states (DOS), measured from neutron scattering on LSCO (Fig. 2c)[12], in the sense of the number of modes and their positions. This similarity between the extracted fine structure and the measured phonon features favors phonons as the nature of bosons involved in the coupling with electrons. In this case, in addition to the half-breathing mode at 70~80 meV that we previously considered strongly coupled to electrons[2], the present results suggest that several lower energy optical phonons of oxygens are also actively involved.

For conventional metals, the MEM procedure can be used to extract the Eliashberg function which gives spectral features of the electron-phonon coupling[10]. For strongly correlated cuprate superconductors, *a priori* it is unclear whether the Eliashberg formalism is applicable or not. However, we note that the nodal excitation of LSCO in the normal state may provide a closest case for the procedure to be applicable. Recent transport measurements reveal that a quasiparticle picture may be still reasonable for electrons near the nodal direction, even for very low doping[13]. This is consistent with the ARPES data which show a well-defined peak in the nodal spectra in the lightly doped samples[3]. The nodal dispersion does not have pronounced curvature in its bare band, unlike the strong curvature near the saddle point of the antinodal region. The selection of the nodal direction in the normal state also minimizes complications due to the existence of a superconducting gap or pseudogap in the

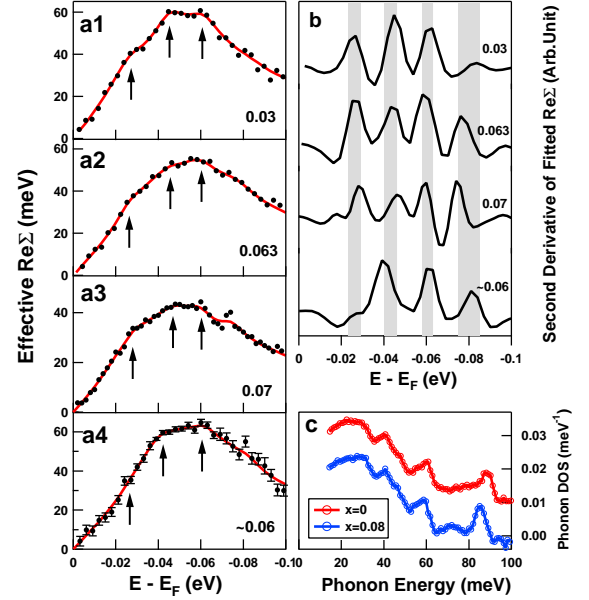


FIG. 2: (a). The effective real part of the electron self-energy for LSCO  $x=0.03$  (a1),  $0.063$  (a2),  $0.07$  (a3) and  $\sim 0.06$  (a4) samples. Data (a1-a3) were taken using Scienta 2002 analyzer, 10eV pass energy at an overall energy resolution (convoluted beamline and analyzer resolution) of  $\sim 18$  meV. Data (a4) were taken using Scienta R4000 analyzer, 5eV pass energy at an overall energy resolution of  $\sim 12$  meV. For clarity, the error bar is only shown for data (a4) which becomes larger with increasing binding energy. The arrows in the figure mark possible fine structures in the self-energy. The data are fitted using the maximum entropy method (solid red lines). The values of  $(\alpha_1, \alpha_2)$  (the unit of  $\alpha_1$  and  $\alpha_2$  are  $\text{eV} \cdot \text{\AA}$  and  $\text{eV} \cdot \text{\AA}^2$ , respectively) for bare band are  $(-4.25, 0)$  for (a1),  $(-4.25, 13)$  for (a2),  $(-3.7, 7)$  for (a3) and  $(-4.3, 0)$  for (a4). (b). The second-order derivative of the calculated  $\text{Re}\Sigma$ . The ruggedness in the curves is due to limited discrete data points. The four shaded areas correspond to energies of (23~29), (40~46), (58~63) and (75~85) meV where the fine features fall in. (c) The phonon density of state  $F(\omega)$  for LSCO  $x=0$  (red) and  $x=0.08$  (blue) measured from neutron scattering[12].

extraction process.

Given these considerations and the fact that there is no better alternative available, we made an attempt by applying the Eliashberg formalism and the MEM procedure to extract the effective bosonic function from the real part of the electron self-energy (Fig. 3a). It is clear that the multiple features are rather robust against the choice of the bare band by varying  $\alpha_1$  and  $\alpha_2$ . All other tests as detailed in [10] have been carried out. The fine structure as obtained from LSCO  $x=0.03$  is in agreement with that in the second-order derivative shown in Fig. 2b. The calculated real part of the electron self-energy is plotted in Fig. 3a together with the measured data. Fig. 3b shows the MDC width which is directly related to  $\text{Im}\Sigma = (\Gamma/2)v_0$ , with  $\Gamma$  being the MDC width (Full-Width-at-Half-Maximum, FWHM) and  $v_0$  the bare

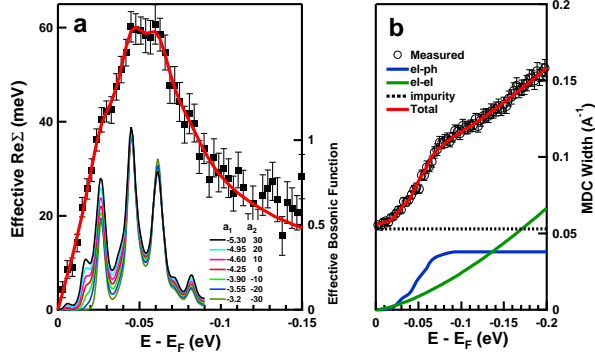


FIG. 3: (a) Real part of the electron self-energy for LSCO  $x=0.03$  as obtained from the dispersion shown in Fig. 1c1 (solid square) and calculated from the extracted effective bosonic spectral using the MEM procedure (red solid curve) with  $\alpha_1=-4.25$  and  $\alpha_2=0$ . Also plotted are the effective bosonic functions obtained by using different bare bands as represented by the different sets of  $\alpha_1$  and  $\alpha_2$  values. (b) The MDC width of LSCO  $x=0.03$  (open circles). The contribution from the electron-phonon coupling (blue line) is calculated from the effective bosonic function in Fig. 3a with  $\alpha_1=-4.25$  and  $\alpha_2=0$ . The “impurity” contribution is assumed to be a constant,  $0.053 \text{ \AA}^{-1}$  (dotted black line). The momentum resolution here is  $0.019 \text{ \AA}^{-1}$ . After subtracting all the electron-phonon and “impurity” contributions, the residual part is fitted by  $C\omega^\alpha$  with  $C\sim 0.7$  and  $\alpha\sim 1.5$  (green line).

velocity. While there is a drop near 75 meV, there is an overall increase of the MDC width with increasing binding energy (Fig. 3b), which is different from simple electron-phonon coupling systems such as Be[8]. The MEM analysis allows us to calculate the contribution of the electron-phonon coupling which gives rise to the abrupt drop in  $\text{Im}\Sigma$ . We note that this calculation has some uncertainty related to the bare band selection (Fig. 3a). After subtracting the contributions from the electron-phonon coupling, “impurity” scattering, and angular resolution, the residual part is found to be proportional to  $\omega^\alpha$  (Fig. 3b). This term most likely represents the contribution of the electron-electron interaction. The corresponding electron-electron contribution in the real part of the self-energy is a smooth function and may be absorbed into the “bare dispersion” because we focus only on abrupt structure in  $\text{Re}\Sigma$  in extracting the bosonic spectral function. Here we also note that while the imaginary part of the electron self-energy is consistent with the existence of electron-phonon coupling, it is difficult to identify the fine structure as has been done for the real part because of the larger experimental uncertainty in determining the peak width over the peak position. This analysis also shows that there is an internal consistency in the MEM procedure that connects the real and imaginary parts of the self-energy.

In summary, by taking high resolution data on heavily underdoped LSCO samples with high statistics, we have

detected fine structure in the electron self-energy. This indicates multiple bosonic modes are involved in the coupling to electrons in the LSCO system.

The work at the ALS and SSRL is supported by the DOE’s Office of BES, Division of Material Science, with contract DE-FG03-01ER45929-A001 and DE-AC03-765F00515. The work at Stanford was also supported by NSF grant DMR-0304981 and ONR grant N00014-04-1-0048-P00002. EWP is supported by DOE DMS and NSF-DMR-0451163. The work at Oak Ridge National Laboratory was partially supported through DOE under Contract DE-AC05-00OR22725. The work in Japan is supported by a Grant-in-Aid from the Ministry of Education, Culture, Sports, Science and Technology of Japan and the NEDO. The work in China is supported by NSF of China and Ministry of Science and Technology of China through Project 10174090 and Project G1999064601.

- 
- [1] A. Damascelli, Z.-X. Shen and Z. Hussain, *Rev. Mod. Phys.* **75** (2003) 473.
  - [2] A. Lanzara et al., *Nature (London)* **412**, 510(2001).
  - [3] X. J. Zhou et al., *Nature (London)* **423**, 398 (2003); X. J. Zhou, et al., *Phys. Rev. Lett.* **92** 187001(2004); T. Yoshida et al., *Phys. Rev. Lett.* **91**, 027001 (2003).
  - [4] A. Kaminski et al., *Phys. Rev. Lett.* **86**, 1070 (2001); P. D. Johnson et al., *Phys. Rev. Lett.* **87**, 177007 (2001); S. V. Borisenko et al., *Phys. Rev. Lett.* **90**, 207001 (2003).
  - [5] J. M. Rowell et al., *Phys. Rev. Lett.* **10**, 334 (1963); D. J. Scalapino et al., *Phys. Rev.* **148**, 263 (1966).
  - [6] S. Komiya et al., *Phys. Rev. B* **65**, 214535 (2002); F. Zhou et al., *Supercon. Sci. Technol.* **16**, L7 (2003).
  - [7] A. W. Sandvik et al., *cond-mat/0309171*; T. P. Devereaux et al., *Phys. Rev. Lett.* **93**, 117004 (2004).
  - [8] S. Lashell et al., *Phys. Rev. B* **61**, 2371(2000).
  - [9] From the simulations we have done, a finite momentum resolution has little effect on the fine structures in the dispersion extracted from the MDC method. High energy resolution is important to identify the fine structures.
  - [10] J. R. Shi et al., *Phys. Rev. Lett.* **92**, 186401 (2004).
  - [11] The spin excitation spectrum of LSCO  $x=0.14$  shows a broad peak at a lower energy ( $\sim 20$  meV) (S. M. Hayden et al., *Phys. Rev. Lett.* **76**, 1344 (1996)). This peak is pushed down to below 5 meV in LSCO  $x=0.07$  (H. Hiraka et al., *J. Phys. Soc. Jpan* **70**, 853 (2001)) and in  $x=0.05$  (H. Goka *Physica C* **388-389**, 239(2003)). A measurement from stripe ordered  $\text{La}_{1.875}\text{Ba}_{0.125}\text{CuO}_4$  and related calculation showed a broad feature centered around 50~60 meV (Tranquada et al., *Nature* **429**(2004)534). Given that this is a different material at different doping, we do not consider this as relevant to the LSCO  $x=0.03\sim 0.07$ . The rapid change of spin spectra with doping has also been observed in  $\text{YBa}_2\text{Cu}_3\text{O}_{7-\delta}$ , S. Chakravarty et al., *Phys. Rev. B* **63**, 094503 (2001)).
  - [12] R. J. McQueeney et al., *Phys. Rev. Lett.* **87**, 077001 (2001); L. Pintschovius and M. Braden, *Phys. Rev. B* **60**, R15039 (1999).
  - [13] Y. Ando et al., *Phys. Rev. Lett.* **87**, 017001 (2001).